Infrared transmission study of crystal-field excitations in $Sm_{1+x}Ba_{2-x}Cu_3O_{6+y}$

D. Barba and S. Jandl
Centre de recherche sur les propriétés électroniques des matériaux avancés, Département de physique, Université de Sherbrooke, Sherbrooke, Canada J1K 2R1

V. Nekvasil and M. Maryško
Institute of Physics, Czech Academy of Sciences, Cukrovarnická 10, 162 53 Praha 6, Czech Republic

M. Diviš
Department of Electron Systems, Charles University, Ke Karlovu 2, 121 16 Praha 2, Czech Republic

A. A. Martin,* C. T. Lin, and M. Cardona
Max Planck Institut für Festkörperforschung, Heisenbergstrasse 1, D-70569 Stuttgart, Germany

T. Wolf
Institut für Festkörperphysik, D-76021 Karlsruhe, Germany
(Received 28 July 2000; published 17 January 2001)

Absorption bands, corresponding to the crystal-field (CF) excitations of the Sm^{3+} ions in $SmBa_2Cu_3O_6$, have been observed by infrared transmission spectroscopy and assigned to transitions from the lowest energy levels of the $^6H_{5/2}$ multiplet to the excited multiplets $^6H_{7/2}$, $^6H_{9/2}$, $^6H_{11/2}$, $^6H_{13/2}$, $^6F_{7/2}$, and $^6F_{9/2}$ of Sm^{3+} ions on the regular D_{4h}-symmetry sites and the C_{4v}-symmetry Ba sites. A set of the CF parameters that fits the levels in the regular sites and reproduces the magnetic susceptibility anisotropy has been derived. The CF interaction parameters in the Sm/Ba sites have been modeled by combining the superposition model and an *ab initio* method based on the density-functional calculations.

DOI: 10.1103/PhysRevB.63.054528 PACS number(s): 74.72.Jt, 78.30.Hv, 75.10.Dg, 71.70.Ej

I. INTRODUCTION

Infrared absorption and electronic Raman spectroscopy have been successfully used in the study of intermultiplet crystal-field (CF) excitations in rare-earth (RE) based cuprates of the $(RE)_{2-x}Ce_xCuO_4$ (RE = Nd, Sm, Pr, $x=0.00$ and 0.15) family[1–4] in spite of the widespread belief that optical techniques are not appropriate to study rare-earth electronic f-f transitions in opaque materials.[5,6] Besides pure CF transitions, Raman active coupled phonon-CF excitations, in $NdBa_2Cu_3O_{7-\delta}$ (Ref. 7) and $SmBa_2Cu_3O_{7-\delta}$,[8] have been reported. Recently, absorption bands corresponding to Nd^{3+} CF excitations in $NdBa_2Cu_3O_6$ have been observed by infrared spectroscopy and assigned to transitions between CF levels of the $^4I_{9/2}$ ground state to the excited multiplets $^4I_{11/2}$, $^4I_{13/2}$, and $^4I_{15/2}$ of Nd^{3+} ions on the regular rare-earth site and on the Ba sites.[9]

The RE ions in high-T_c superconductors and related compounds occupy sites adjacent to the CuO_2 planes where the charge carriers responsible for superconductivity are located. Hence CF excitations that probe the charge distribution in the CuO_2 planes and the structural changes induced by doping have been studied extensively by inelastic neutron scattering on polycrystalline samples.[10] However, such measurements have succeeded to observe only a small number of CF excitations which is generally insufficient for a precise determination of the CF parameters that appear as prefactors of the spherical tensor operators of the CF Hamiltonian.[11] Raman spectroscopy and infrared absorption, which can be applied with high resolution in the study of small single crystals without limitation to the low energies CF excitations, thus complement remarkably the initial neutron studies.

Sm^{3+} CF excitations in $SmBa_2Cu_3O_7$ have been studied by inelastic neutron scattering.[12] In order to avoid the large neutron cross section of natural samarium the isotope ^{154}Sm was used. The ordering in energy of CF states in the ground state $^6H_{5/2}$ and in the first excited $^6H_{7/2}$ multiplet was assigned. A set of CF parameters has been derived and the need for measurements beyond the first excited multiplet has been expressed.

In this paper we report a systematic study, combining the infrared absorption measurements with various theoretical approaches, of CF transitions in $Sm_{1+x}Ba_{2-x}Cu_3O_{6+y}$ ($y \sim 0$) samples from the lowest energy levels of the $^6H_{5/2}$ multiplet to the $^6H_{7/2}$, $^6H_{9/2}$, $^6H_{11/2}$, $^6H_{13/2}$, $^6F_{7/2}$, and $^6F_{9/2}$ excited multiplets. The CF fits to the infrared spectra allow us to account for the observed anisotropy of the magnetic susceptibility.

II. EXPERIMENT

$Sm_{1+x}Ba_{2-x}Cu_3O_{6+y}$ single crystals were grown by the self-flux method with ($x \leqslant 0.01$, $x=0.05$, and 0.11) as described in Ref. 13 and with ($x=0.03$) according to Ref. 14. They were subsequently annealed in high-vacuum at 700 °C for four days. The value of x was estimated from the nominal Sm/Ba ratio in $BaCO_3$, Sm_2O_3, and CuO flux mixtures and checked by energy-dispersive x ray for $x=0.01$, 0.05, and 0.11. Deviations from the nominal composition were less than 1%.

The infrared measurements were carried out with a Fourier-transform interferometer (BOMEM DA3.002) using either a globar source, an MCT detector, and a KBr beam splitter in the 900–2000-cm^{-1} range, or a quartz halogen lamp, an InSb detector, and a CaF_2 beam splitter in the 1800–10 000-cm^{-1} range. The $Sm_{1+x}Ba_{2-x}Cu_3O_{6+y}$ single crystals, with approximate dimensions of $1.5\times1.5\times0.1$ mm^3, were mounted on a cold finger of a helium-cooled flow-through cryostat and 1-cm^{-1} resolution transmittance measurements were performed with the *ac* plane perpendicular to the direction of the unpolarized incident beam. The spectra were measured over the temperature range from 8 to 300 K.

The magnetic susceptibility of single crystalline platelets having a mass between 20 and 60 mg has been measured, one at a time, using a superconducting quantum interference device magnetometer Quantum Design MPM-5S in the temperature range from 4.5 to 300 K. The static magnetic field of 0.1 T was oriented parallel and perpendicular to the CuO_2 layers.

III. THEORETICAL BACKGROUND

Interaction with the crystal field produced by the neighboring core charges and the valence electronic charge density is the strongest perturbation of the free ion $4f$ shell state of trivalent RE ions in cuprates. The interaction Hamiltonian can be written as

$$H_{CF}=\sum_{k,q} B_{kq}[C_q^{(k)}+C_{-q}^{(k)}], \tag{1}$$

where the functions $C_q^{(k)}$ transform as tensor operators[11] under simultaneous rotation of the coordinates of all the f electrons, and B_{kq} are the so-called CF parameters. In this work we examine theoretically the CF of Sm^{3+} at regular D_{4h}-symmetry sites and at C_{4v}-symmetry Ba sites in $Sm_{1+x}Ba_{2-x}Cu_3O_6$. In both cases the CF interaction can be described using Eq. (1) containing five nonzero independent parameters B_{20}, B_{40}, B_{44}, B_{60}, and B_{64}. Their values are determined by combining different approaches. In regular Sm^{3+} sites we calculate the unknown parameters B_{kq} solving numerically the *inverse secular problem*, where the experimental CF energy levels are taken to be the eigenvalues of the secular equation of H_{CF}.

To predict the $k=4$ and 6 CF parameters of Sm^{3+} at Ba sites we use the superposition model[15] proved to be efficient in the CF modeling.[16] The model, introduced to separate the geometrical and physical information contained in the CF parameters, allows us to describe the CF parameters B_{kq} in Eq. (1) in terms of intrinsic (pair) CF parameters $b_k(R)$ where R denotes the distance between the RE and ligand ion as

$$B_{kq}=\sum_i S_{kq}(i)\cdot b_k(R_i), k=4,6, \tag{2}$$

where $S_{kq}(i)$ is the geometrical factor determined by angular coordinates of ligands at the same distance R_i. A standard way of expressing the dependence of the intrinsic parameters on distance is to assume the power-law dependence:

$$b_k=b_k(R_0)\cdot(R_0/R)^{t_k}. \tag{3}$$

The superposition model is rather unaccurate for the second-order parameters for which the long-range electrostatic contributions appear to dominate. This causes a breakdown of one of the postulates of the superposition model.[15] Therefore to calculate B_{20} we use an *ab initio* method recently applied to RE cuprates.[17] Within this method the electronic structure and the corresponding distribution of the ground-state charge density in the studied compounds are obtained from the first-principle calculations based on the density-functional theory (DFT). Exchange and correlation effects are treated within the local spin-density approximation (LSDA) and the generalized gradient approximation (GGA).[18] The scalar relativistic Kohn-Sham equations are used to obtain the self-consistent single electron wave functions. The calculations described in Sec. IV were performed using the full potential linearized augmented plane-wave method (LAPW) implemented in the latest version of the original WIEN code.[19] Atomic sphere radii of 2.8, 2.0, 1.9, and 1.5 a.u. were taken for Sm, Ba, Cu, and O, respectively. The basis functions were represented by 1500 plane waves (more than 100 APW/atom) plus local orbitals of Sm ($5s$, 5), Ba ($5s$, 5), Cu ($3p$), and O ($2s$) semicore states, which lie less than 6 Ry below the Fermi level. A maximum of $l=12$ was adopted for the expansion of the radial wave function. Inside the spheres the crystal potential and charge density were expanded into crystal harmonics up to the sixth order. For the Brillouin zone integrations a tetrahedron method[19] with 40–50 special **k** points was used. The remaining computational details were very similar to those in Ref. 20.

The Sm $4f$ states in the spherical part of the potential are treated as atomiclike core states (open-core treatment, see Ref. 21). Sm^{3+} in the studied compounds is characterized by the integer occupation number $N_{4f}=5$. A similar approach was successfully used in the DFT calculations for $PrBa_2Cu_3O_6$.[20] Within the DFT the parameter B_{20} of the CF Hamiltonian, Eq. (1), originating from the effective potential V inside the crystal, can be written as

$$B_{20}=a_2^0\int_0^\infty |R_{4f}(r)|^2 V_2^0(r) r^2 dr, \tag{4}$$

where the nonspherical component $V_2^0(r)$ reflects besides the nuclear potentials and Hartree part of the interelectronic interaction and also the exchange correlation term which accounts for many-particle effects. The radial wave function R_{4f} describes the radial shape of the localized $4f$ charge density of Sm^{3+} ion in the studied compounds. It is well known that the use of self-consistent +open core; R_{4f} leads to a poor description of the CF interaction. The reason is that the so-called +self-interaction; potential felt by a localized $4f$ electron is not correctly treated within the LSDA.[21] Therefore the present study uses the value of the R_{4f} in Eq. (4) resulting from the self-interaction corrected (SIC) LSDA

atomic calculations with occupation numbers of the valence electrons of the Sm ($6s$, $5d$, $6p$) fixed to their values obtained in the selfconsistent LSDA calculations in a given Sm compound. This approach[22] was found to give a $4f$ charge density which is very close to that obtained from more rigorous DFT band calculation which includes SIC for the $4f$ states directly.[21]

To calculate $V_2^0(r)$ we rewrite the right-hand side of Eq. (4) as a sum of two contributions,

$$B_{20}=a_2^0\left\langle \int_0^{R_{MT}}|R_{4f}(r)|^2U_2^0(r)r^2dr + \int_{R_{MT}}^{\infty}|R_{4f}(r)|^2W_2^0(r)r^2dr\right\rangle, \quad (5)$$

where $U_2^0(r)$ and $W_2^0(r)$ are respectively the components of the effective potential inside the atomic sphere with radius R_{MT} and in the interstitial region. The term $U_2^0(r)$ is readily obtained with the above-mentioned (LAPW) code. The most interesting feature of our approach is that $W_2^0(r)$ is calculated using the exact transformation of the interstitial plane-wave representation of the potential into the spherical Bessel functions. The conversion factor $a_2^0=\sqrt{5/4\pi}$ establishes the relation between the LAPW symmetrized spherical harmonic and the real tesseral harmonics which transform in the same way as tensors operators $C_q^{(k)}$ in Eq. (1).

In our CF calculations reported in Sec. IV the matrix of the operator H_{CF} [Eq. (1)] is diagonalized within a truncated basis set which includes the 12 lowest J multiplets, using the same free ion intermediate coupling wave functions and energies as in our similar study of Sm_2CuO_4.[4] Justification of such a truncation is provided by our very good reproduction of the CF splitting of these 12 multiplets for Sm^{3+} in $LiYF_4$, calculated considering a basis set which includes the 30 lowest J multiplets.[23]

The principal values of the paramagnetic susceptibility tensor χ_a in a magnetic field **H** applied along the a axis are calculated using the formula

$$\chi_a=\left(\frac{\delta m_\alpha}{\delta H_\alpha^a}\right)_{H^a\to 0}, \quad (6)$$

where m_α represents the thermal average of the Sm^{3+} magnetic moment calculated using standard Boltzmann statistics. To evaluate this moment, the Zeeman term

$$H_{Zeem}=\mu_B(\mathbf{L}+\mathbf{g_s}\mathbf{S})\cdot\mathbf{H^a} \quad (7)$$

was included in the perturbation Hamiltonian and the combined CF and Zeeman matrices were simultaneously diagonalized.

IV. RESULTS AND DISCUSSION

When the Sm^{3+} ion is placed in a tetragonal symmetry site, as in $SmBa_2Cu_3O_6$, the ground-state manifold $^6H_{5/2}$ splits into three Kramers degenerate doublets while the higher multiplets, $^6H_{7/2}$, $^6H_{9/2}$, $^6H_{11/2}$, and $^6H_{13/2}$, split into four, five, six, and seven Kramers doublets, respectively. The observation of infrared-active CF bands within Sm^{3+} ions placed at the inversion center (the regular D_{4h}-symmetry site in $SmBa_2Cu_3O_6$) is electric dipole forbidden. We conjecture that these bands become observable due to slight lattice imperfections related to a small amount of Sm^{3+} ions in the Ba sites or to oxygen nonstoichiometry as verified in the study of the Nd^{3+} infrared (IR) active CF excitations in $NdBa_2Cu_3O_6$.[9]

Figures 1(a) and 1(b) show the IR transmission spectra of the $Sm_{1+x}Ba_{2-x}Cu_3O_{6+y}$ single crystals, obtained at 8 K, in the 950–1550-cm^{-1} spectral range where the $^6H_{5/2}\to{}^6H_{7/2}$ transitions occur. In the $x=0.01$ sample, CF doublets and three CF excitation bands of the four expected excitations for the $^6H_{7/2}$ multiplet in regular sites are observed at 974/981, 1326/1334, and 1460 cm^{-1}, respectively. They show a tendency to broaden in the substituted ($x>0.01$) samples. In all samples, bands of phononic origin[24] are detected and indicated by asterisks. We note the presence of water vapor absorption bands around 1250 cm^{-1} (black circle) which mask the observation of the CF excitation in this range.

Figures 2(a) and 2(b) correspond to the $^6H_{5/2}\to{}^6H_{9/2}$ IR transitions in the 2150–2700-cm^{-1} range at 8 K. CF excitations at 2207, 2388, 2533, and 2644 cm^{-1} are observed in the ($x=0.01$) and in the ($x>0.01$) $Sm_{1+x}Ba_{2-x}Cu_3O_{6+y}$ single crystals where an additional CF excitation is observed at 2299 cm^{-1}. We also observe bands around 2410 and 2450 cm^{-1} whose dependence on x and temperature strongly differs from that of the other CF excitations. Since these absorption bands are also present in the $NdBa_2Cu_3O_6$ spectra,[9] we associate them with either a lattice defect or magnetic excitations, common to the $RE_{1+x}Ba_{2-x}Cu_3O_{6+y}$ compounds.

$^6H_{5/2}\to{}^6H_{11/2}$ transitions, which cover the 3500–4000-cm^{-1} range, are shown in Figs. 3(a) and (b) for T = 8 K. CF excitations at 3531, 3561, 3571, 3791, 3815, and 3953/3970 cm^{-1} are common to all the samples with an increased broadening in the ($x>0.01$) samples. Also in the latter samples, additional CF excitations are observed around 3620 cm^{-1}.

Figures 4(a) and (b) present the $^6H_{5/2}\to{}^6H_{13/2}$ transitions in the 4850–5050 and 5150–5400 cm^{-1} ranges, respectively, at 8 K. CF excitations at 4860, 4871, 5025/5034, 5261, 5282, 5306, and 5329 cm^{-1} are observed in the ($x=0.01$) sample while new bands are detected around 4898 and 4950 cm^{-1} in the ($x=0.05$) sample.

In Figs. 5(a)–(e), CF excitations at 8 and 78 K are shown. They allow the determination of the ground-state excited levels[8] at 92 and 192 cm^{-1} and show CF excitations in the 8050–8350- and 9110–9400-cm^{-1} ranges.

It appears natural to associate the IR absorption bands common to the ($x=0.01$) and ($x>0.01$) samples with the Sm^{3+} ions at regular D_{4h}-symmetry sites and the additional IR absorption bands, in the ($x>0.01$) samples, with Sm^{3+} ions at the C_{4v} symmetry Ba sites. To examine more rigorously the origin of the individual bands we have performed a detailed CF analysis described in the following.

In a first step, using the numerical procedure described in

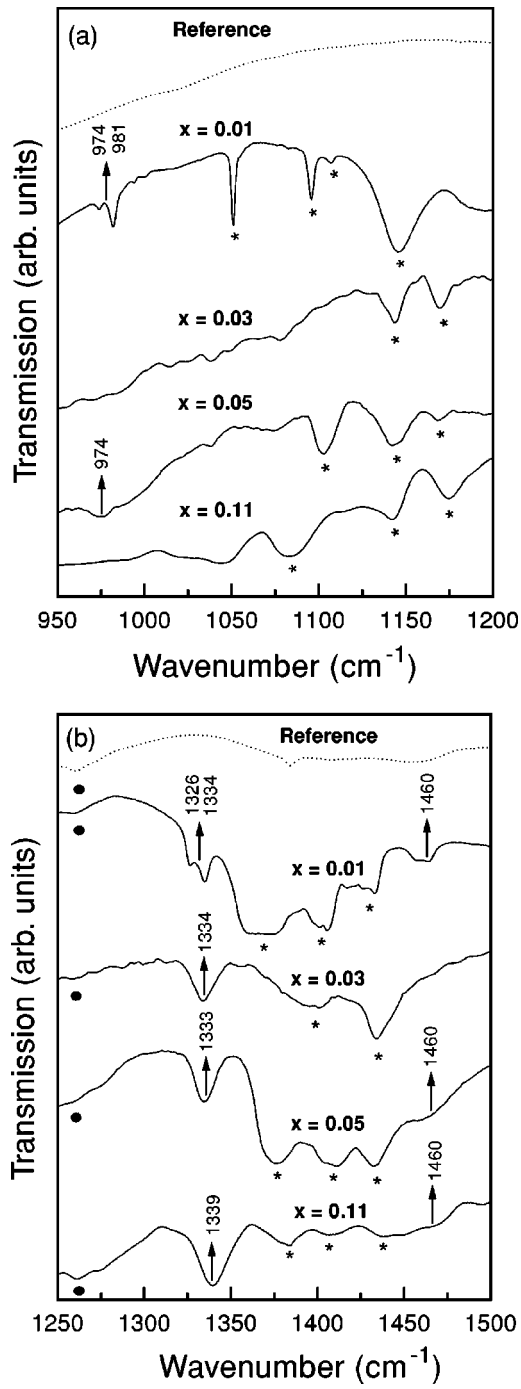

FIG. 1. IR transmission spectra at $T=8$ K across ac-oriented platelets of $Sm_{1+x}Ba_{2-x}Cu_3O_{6+y}$. (a) and (b) show the 950–1200-cm^{-1} and 1250–1500-cm^{-1} ranges, respectively. Arrows correspond to $^6H_{5/2}\rightarrow{}^6H_{7/2}$ transitions, (*) designates excitations of phononic origin, and (●) is associated with a water vapor absorption.

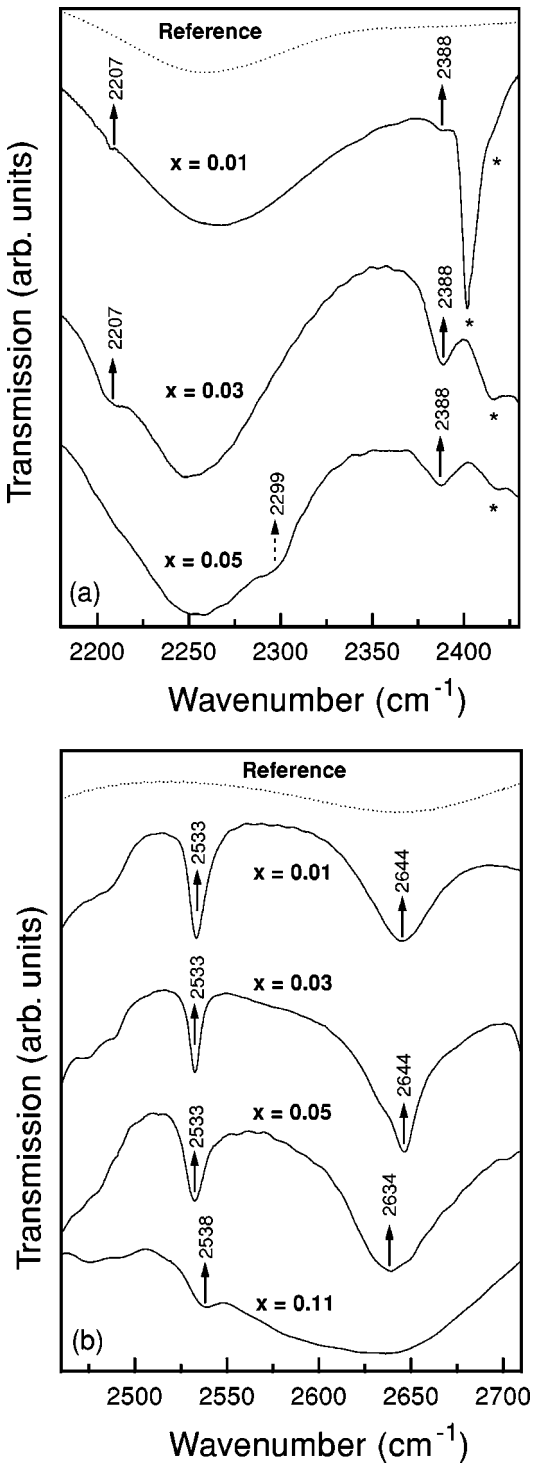

FIG. 2. IR spectra of the $^6H_{5/2}\rightarrow{}^6H_{9/2}$ CF transitions (arrows) in $Sm_{1+x}Ba_{2-x}Cu_3O_{6+y}$ in the 2175–2450-cm^{-1} (a) and 2430–2720-cm^{-1} (b) ranges, respectively. The dashed arrow indicates a CF excitation associated with Sm on the C_{4v}-symmetry Ba site and (*) represents absorption bands also observed in $NdBa_2Cu_3O_6$.

Sec. III, with the CF parameters in the regular Nd sites[9] in $NdBa_2Cu_3O_6$ serving as an initial estimate, we fitted transitions within the two lowest J multiplets where no ambiguity appears in the identification of the origin of individual peaks in the spectra due to the presence of their electronic replica at 92 cm^{-1}. In a second step, we included in the input data only well isolated experimental levels within the second excited multiplet, if they were simultaneously close to levels predicted using the CF parameters from the previous fit. This procedure was iterated till the levels of the fourth excited multiplet $^6H_{13/2}$ were included. The final best-fit parameters for regular D_{4h}-symmetry sites are given in Table I; the free

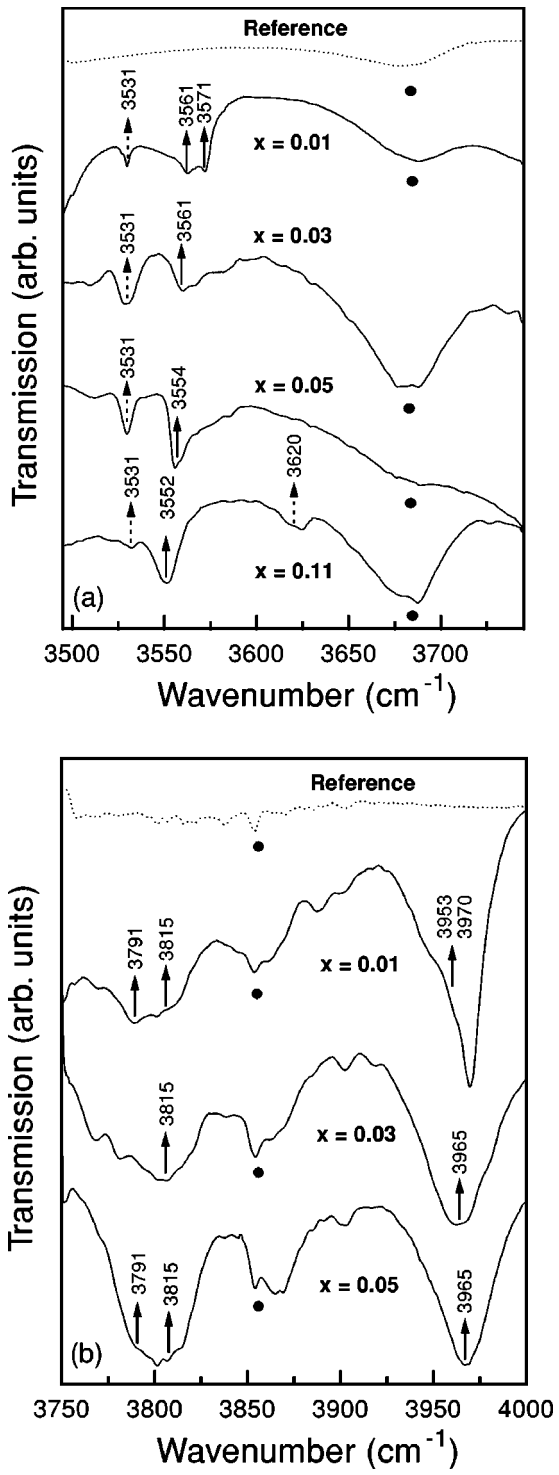

FIG. 3. IR spectra of the ${}^6H_{5/2}\rightarrow{}^6H_{11/2}$ CF transitions for regular sites (arrows) and Sm/Ba sites (dashed arrows) in $Sm_{1+x}Ba_{2-x}Cu_3O_{6+y}$ in the 3500–3750-cm^{-1} (a) and 3750–4000-cm^{-1} (b) ranges, respectively. (●) corresponds to CO_2 and water vapor absorptions in (a) and (b), respectively.

ion levels of the lowest five multiplets, varied along with the CF parameters in the fitting procedure are 0, 1049, 2248, 3563, and 4938 cm^{-1}. Table II presents the corresponding experimental and calculated CF levels; good agreement is obtained, with a standard deviation of 3.9 cm^{-1}. A similar

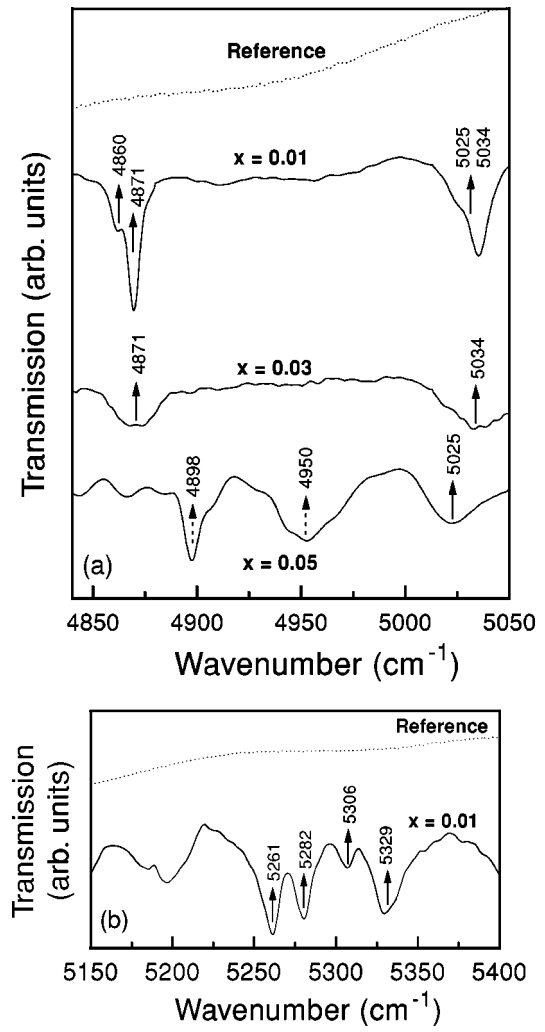

FIG. 4. IR spectra of CF transitions (${}^6H_{5/2}\rightarrow{}^6H_{13/2}$) in $Sm_{1+x}Ba_{2-x}Cu_3O_{6+y}$ in the 4800–5050-cm^{-1} range (a) and in the 5150–5400-cm^{-1} range (b). The dashed arrows indicate CF transitions associated with Sm/Ba sites.

CF study of the two lowest J multiplets, based on inelastic neutron scattering,[12] is available for Sm^{3+} in the orthorhombic $SmBa_2Cu_3O_7$. A comparison of our results with these data is somewhat hampered by an uncertainty in the CF parametrization scheme used. In Eq. (1) of Ref. 12 the CF Hamiltonian is written in terms of spherical tensor operators. The values of the best-fit CF parameters strongly indicate, however, that these parameters are in fact expressed within an alternative Stevens parametrization scheme, commonly used by Guillaume *et al.*[12] If this is the case, then the tetragonal; CF parameters for D_{2h}-symmetry Sm sites in $SmBa_2Cu_3O_7$, expressed within the Wybourne scheme implied in our Eq. (1), take the values given in the fourth column in Table I. These parameters are rather similar to those obtained here for the D_{4h}-symmetry sites, given in the second column in Table I. Also the CF parameters of Sm^{3+}, in $SmBa_2Cu_3O_6$, and Nd^{3+} in $NdBa_2Cu_3O_6$ reported in Table I show a rather smooth variation, as expected across the lanthanide series.[25]

We note that we also have been able to detect a number of

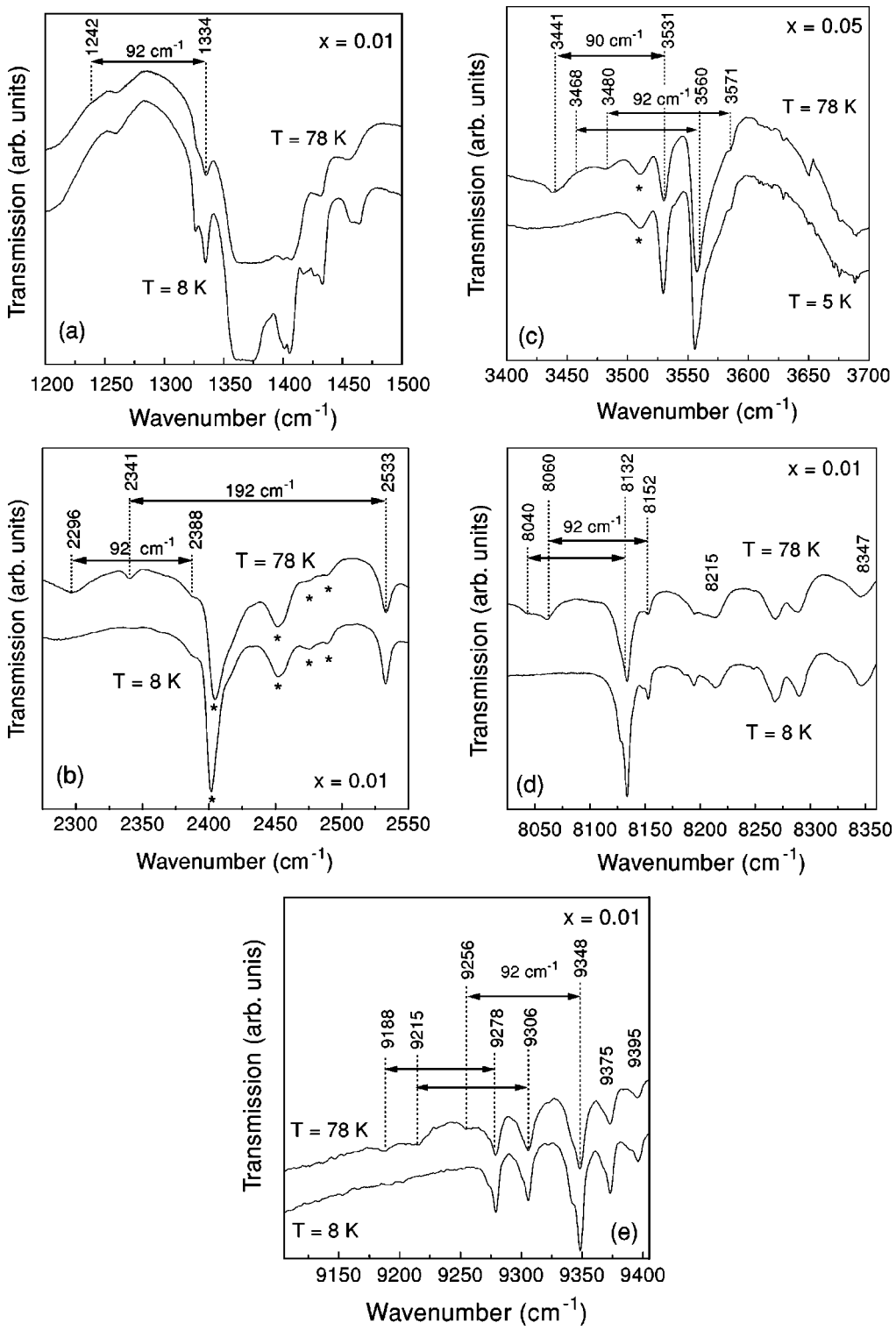

FIG. 5. Comparison between IR transmission measurements at $T=8$ K and $T=78$ K in the 1200–1500-cm^{-1} (a), 2250–2550-cm^{-1} (b), 3400–3700-cm^{-1} (c), 8030–8350-cm^{-1} (d), and 9110–9400-cm^{-1} (e) ranges. (*) indicates, in (b), excitations also observed in $NdBa_2Cu_3O_6$, and an excitation of site symmetry other than D_{4h} and C_{4v} in (c).

IR excitations in the energy range from ~6000 to ~10 000 cm^{-1}. These excitations are particularly difficult to interpret in the energy range from ~6000 to ~7700 cm^{-1} where, in addition to an uncertainty associated with the multiplicity of Sm sites, there is an overlap of the CF spectra of the $^6H_{15/2}$, $^6F_{1/2}$, and $^6F_{3/2}$ multiplets with the $^6F_{5/2}$ multiplet in their close proximity. These facts make the classification of individual peaks ambiguous in the relatively narrow range of energies where we observed experimentally 25 excitations while only 14 are expected from the multiplicity

TABLE I. Sm_{1+x} Ba_{2-x} Cu_3 O_{6+y} crystal-field parameters (in cm^{-1}) obtained from a fit to our IR measurements for Sm^{3+} ions on the regular (D_{4h}) sites and calculated using the superposition model and DFT based *ab initio* calculations for Sm^{3+} on the Ba site (C_{4v}). For comparison, the CF parameters of Nd^{3+} in $NdBa_2Cu_3O_6$ are given in the third and sixth columns.

Parameter	D_{4h} site		D_{2h} site	C_{4v} site	
	This work	Ref. 9	Ref. 12	This work	Ref. 9
B_{20}	282(5)	380	368	−227	0
B_{40}	−2481(12)	−2956	−2562	24	14
B_{44}	1307(10)	1664	1263	−331	−364
B_{60}	321(12)	526	697	−427	−468
B_{64}	1931(6)	2021	1992	624	700

of the J multiplets. This is the reason why we did not include the levels above $\sim$6000 cm^{-1} into the above-mentioned CF analysis as input data. Envisaged are Zeeman experiments which should enable us to unravel the nature of the individual excitations. More reliable is an interpretation of the IR spectra of the relatively isolated multiplets $^6F_{7/2}$ and $^6F_{9/2}$ given in Figs. 5(d) and (e), respectively. The bands at 8132, 8152, 8215, 8347 [Fig. 5(d)], 9278, 9306, 9348, 9375, and 9395 cm^{-1} [Fig. 5(e)], with an eventual replica at 92 cm^{-1}, compare well with the calculated CF splitting, obtained using the CF parameters given in the second column in Table I and allowing for a small shift in free ion energies, with levels at 8139, 8155, 8209, and 8349 cm^{-1} for the $^6F_{7/2}$ multiplet and 9280, 9308, 9342, 9370, and 9401 cm^{-1} for the $^6F_{9/2}$ multiplet. This agreement provides an independent check of reliability of our CF best fit of the lower-energy part of the CF spectra.

To estimate the CF levels for Sm^{3+} placed in C_{4v}-symmetry Ba sites we calculate the Hamiltonian parameters of Eq. (1) using methods introduced in the previous section, considering the available intrinsic model parameters b_k and t_k (Ref. 17) and structural data[26] for $SmBa_2Cu_3O_{6+y}$. The CF parameters of fourth and sixth order in the fifth column of Table I were calculated using the superposition model. The CF parameter B_{20} for the Sm^{3+} in Ba position were calculated using the DFT-based approach described in

TABLE II. Sm^{3+} CF levels in Sm_{1+x} Ba_{2-x} Cu_3 O_{6+y} crystal (this work) and in $SmBa_2Cu_3O_7$ (Ref. 12), and the corresponding energies obtained from a fit of the CF Hamiltonian [Eq. (1)] to the data (see Table I). The CF levels for D_{4h} and C_{4v} are for the Sm^{3+} ion on the regular site and the Ba site, respectively.

	Experiment			Theory			
	Ref. 12	This work		Ref. 12	This work		
Multiplet	D_{2h} site (cm^{-2})	D_{4h} site (cm^{-2})	C_{4v} site (cm^{-1})	D_{2h} site (cm^{-2})	D_{4h} site (cm^{-1})	Sym. (D_{4h}) i (Γ_i)	C_{4v} site (cm^{-1})
	0	0	0	0	−5	6	0
$^6H_{5/2}$	97	92		97	94	7	72
	194	192	90	189	195	7	92
	999	974/981 [a]		994	979	6	1029
	1244			1242	1255	7	1063
$^6H_{7/2}$	1352	1326/1334 [a]		1355	1336	7	1153
	1488	1460		1473	1453	6	1208
		2207			2205	6	2217
		2388	2299		2389	7	2257
$^6H_{9/2}$					2495	6	2325
		2533			2532	7	2335
		2644			2646	6	2400
		3561	3531		3562	6	3526
		3571			3569	7	3601
$^6H_{11/2}$		3791			3793	7	3602
		3815	3620		3813	6	3613
					3889	6	3695
		3953/3970 [a]			3962	7	3708
		4860	4898		4862	6	4911
		4871	4950		4871	7	4947
		5025/5034 [a]			5029	7	4954
$^6H_{13/2}$		5261			5257	6	4969
		5282			5280	7	4981
		5306			5309	7	5042
		5329			5332	6	5045

[a]The doublet energies are approximated by their average value.

Sec. III. The task was to solve the case when the impurity Sm atom are placed in $(0.5,0.5,z_{Ba})$ positions in the otherwise ideal $SmBa_2Cu_3O_6$ crystal structure. It requires the construction of very large supercells, at least 30 times larger than the elementary cell, in the ideal structure $SmBa_2Cu_3O_6$, i.e., it includes several hundreds atoms. To our knowledge, the successful full-potential DFT calculations reported so far do not go beyond ~ 100 atoms in the primitive cell. Therefore to calculate B_{20} in Ba sites we introduced in the present study the artificial crystal structure $Ba(Ba,Sm)_2Cu_3O_6$ in which Sm is in $(0.5,0.5,z_{Ba})$ positions and Ba occupies $(0.5,0.5,1-z_{Ba})$ and (0.5,0.5,0.5) positions.

An important feature of this artificial structure is that the nearest- and the next-nearest-neighbor coordinations are the same as in the ideal supercell. In particular, for the Sm atom located in the $(0.5,0.5,z_{Ba})$ position there are four oxygens O_I at the same distance $R(\text{Sm-O}_I)=278$ Å and four oxygens O_{II} with $R(\text{Sm-O}_{II})=289$ Å; the next-nearest-neighbor copper shell is composed of 4 Cu_{II}, $R(\text{Sm-Cu}_{II})=337$ Å, and 4 Cu_I, $R(\text{Sm-Cu}_I)=355$ Å. The local point-group symmetry of the $(0.5,0.5,z_{Ba})$ site differs in the ideal and artificial structures and the coordination shells start to differ beyond $R=360$ Å. Our numerical simulations have shown, however, that these differences do not influence the final value of B_{20} considerably. Therefore we believe that our value of $B_{20}=-227$ cm^{-1}, obtained using Eq. (5) for the artificial structure $Ba(Ba,Sm)_2Cu_3O_6$, is a meaningful estimate of this parameter for Sm in Ba sites in $SmBa_2Cu_3O_6$. The relevant calculated radial charge distribution $R_{4f}(r)$, the component of the crystal potential $V_2^0(r)$, and $I(r)$, representing the integrand on the right-hand side of Eq. (5), are shown in Figs. 6(a), (b), and (c), respectively.

To check the internal consistency of our DFT method we have also performed the calculations for regular $SmBa_2Cu_3O_{6+y}$ with $y=1$ and $y=0$. The obtained total and atom-projected densities of electronic states are in excellent agreement with the data found in the literature for $YBa_2Cu_3O_7$.[27] Using Eq. (5) for $SmBa_2Cu_3O_6$ we obtained $B_{20}=320$ cm^{-1} which is in reasonnable agreement with our best-fit value given in the second column of Table I. The difference in sign between B_{20} in the regular and Ba sites is connected, within our approach, with a difference in the occupation of the p_x, p_y, and p_z orbitals in the $5p$ and $6p$ valence shells as well as of the d_{z^2}, $d_{x^2-y^2}$, d_{xy}, d_{xz}, and d_{yz} orbitals in the $5d$ valence shell. Significant contributions to B_{20} from charges within the atomic sphere are proportional to the quantities ΔN_p and ΔN_d,[28] which are functions of the occupation numbers n: $\Delta N_p=1/2\ (n_x+n_y)-n_z$ and $\Delta N_d=n_{x^2-y^2}+n_{xy}-1/2\ (n_{xz}+n_{yz})-n_{z^2}$. In our case we have obtained ΔN_p equal to -0.008 and 0.011 electrons and ΔN_d equal to -0.017 and -0.001 electrons for Sm^{3+} ions in the regular and Ba sites, respectively.

To further test the reliability of our DFT-based CF calculations, we have also performed spin-unpolarized LSDA calculations, including spin-orbit interaction for valence electrons, spin-polarized LSDA calculations ($4f$ electrons as spin-polarized core states) and non-spin-polarized GGA calculations. The relative difference of the resulting CF parameter $\delta B_{20}/B_{20}$ was found to be less than 10% among all above-mentioned cases. The theoretical prediction for the CF excitations at the Ba sites, as well as the experimental levels tentatively associated with these sites, are summarized in Table II.

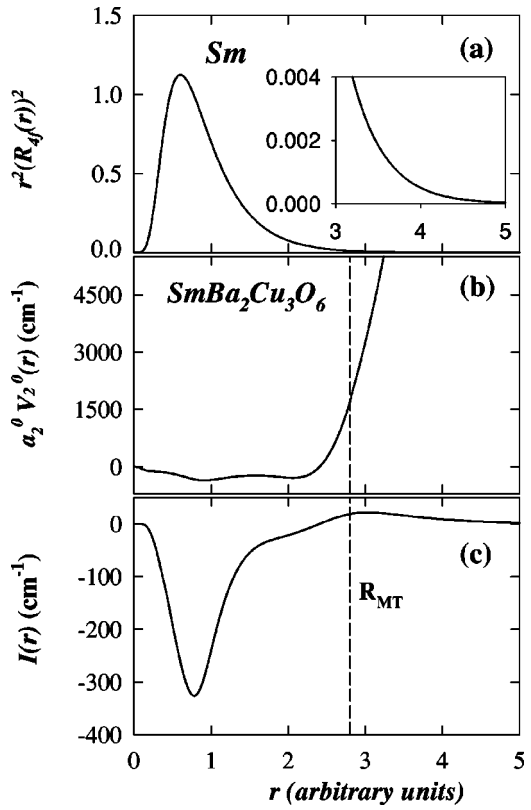

FIG. 6. Calculated radial charge distribution $R_{4f}(r)$ (a), the $a_2^0 V_2^0(r)$ component of the crystal potential (b), and the integrand $I(r)$ on the right-hand side of Eq. (5)(c), as a function of r.

To be noted are doublet features in the IR spectra at 974/981, 1326/1334, 3953/3970, and 5025/5034 cm^{-1} (Table II). In analogy with similar observations in Nd_2CuO_4 we briefly discuss next a possibility that these doublets are due to the Sm-Cu anisotropic exchange interaction. The available dependence of the magnetic specific heat vs temperature for nonsuperconducting $SmBa_2Cu_3O_{6+y}$ ($y\sim 0.5$) is bell shaped with a maximum at ~ 1.07 K. This behavior has been interpreted[29] in terms of a Schottky-type anomaly, suggesting a two-level system for the Sm^{3+} ion with an energy splitting between these levels of about ~ 1.6 cm^{-1}. The first excited CF level in regular sites lies at 92 cm^{-1}. It allows us to tentatively ascribe these two levels to the ground-state Kramers doublet split by a superexchange interaction of $4f$ electrons of Sm with neighboring Cu moments. In the isotropic mean-field approximation this interaction vanishes for symmetry reasons. This implies that the doublet splits due to the anisotropic terms in the Sm-Cu superexchange Hamiltonian. A very similar situation occurs in Nd_2CuO_4 where the splitting of the ground state, as well as that of the excited Kramers doublets, were described by anisotropic terms in an effective exchange Hamiltonian for Nd^{3+} expressed with the help of single electron spherical tensor operators up to the

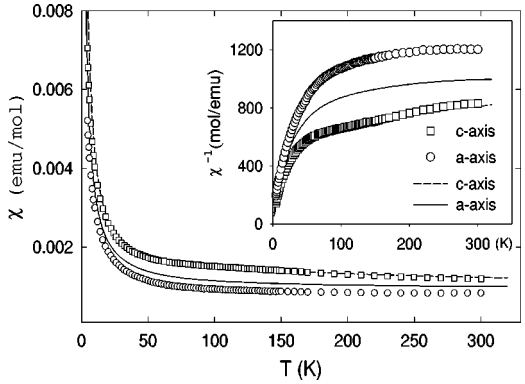

FIG. 7. Magnetic susceptibility measurements (dots) and calculations (lines) in the *a* and *c* directions. Inset: inverse susceptibility.

sixth order.[30] We note that evidence for magnetic coupling between the RE and Cu sublattices is also available in several $REBa_2Cu_3O_{6+y}$ compounds (see, e.g., Ref. 31 and references therein). Envisaged measurement of the CF excitations in $SmBa_2Cu_3O_6$ under external magnetic fields, as previously reported for $NdBa_2Cu_3O_7$,[32] should enable us to determine if the above-mentioned doublet features originate in the anisotropic Sm-Cu coupling or in some local defects.

The paramagnetic susceptibility, calculated using Eq. (7) and the best-fit CF parameters available for regular Sm sites in Table I, is compared in Fig. 7 to experimental data corrected for contribution of the Cu-O subsystem approximated by data available[33] for $YBa_2Cu_3O_{6.05}$. The observation that $\chi_c > \chi_a$ is in agreement with our calculations. The remaining discrepancy between the experimental and the theoretical anisotropy of the magnetic susceptibility is tentatively ascribed to the above-mentioned anisotropic exchange interaction between Sm and Cu, not accounted for in our calculations. To complete the characterization of the magnetic anisotropy induced in $SmBa_2Cu_3O_6$ by the CF interaction we calculated the components of the *g* tensor of the ground-state doublet of Sm^{3+} using the CF parameters for regular sites (Table I): $g_a = 0.52\mu_B$, $g_c = 0.60\mu_B$. An earlier estimate[34] indicates the reversed anisotropy of the *g* tensor: $g_a = 0.63\mu_B$, $g_c = 0.53\mu_B$.

V. CONCLUSION

We have reported a spectroscopic investigation of single crystalline $Sm_{1+x}Ba_{2-x}Cu_3O_{6+y}$ using infrared absorption. We have determined nearly complete CF spectra of the $^6H_{5/2}$, $^6H_{7/2}$, $^6H_{9/2}$, $^6H_{11/2}$, $^6H_{13/2}$, $^6F_{7/2}$, and $^6F_{9/2}$ multiplets of the Sm^{3+} ions in regular D_{4h}-symmetry sites. A CF analysis for these levels gives good account of the experimental data, including the anisotropy of magnetic susceptibility. Theoretical analysis, using the superposition model as well as density-functional based *ab initio* calculations, indicates that some of the additional bands in the infrared spectra arise from the Sm^{3+} ions occupying the C_{4v}-symmetry Ba sites.

ACKNOWLEDGMENTS

We thank J. Rousseau for technical assistance. S.J. acknowledges support from National Science and Engineering Research Council of Canada (NSERC) and le Fond de Formation de Chercheurs et l'aide à la recherche du Gouvernement du Québec. Also gratefully acknowledged are the Grant Agency of the Czech Republic for its Grant Nos. 202/00/1602 and 202/99/184 (V.N., M.M., and M.D.), the Grant Agency of Charles University for Grant No. 145/2000/B-FYZ (M.D.), and FAPESP-Brazil for Grant No. 98/13862-9 (A.A.M.).

*Also at Instituto de Pesquisa e Desenvolvimento, IP&D Univap - São Jose dos Campos, SP Av. Shishima Hifumi, 2911 12.244-000 Brazil.

[1] S. Jandl, P. Dufour, T. Strach, T. Ruf, M. Cardona, V. Nekvasil, C. Chen, B. M. Wanklyn, and S. Pinol, Phys. Rev. B **53**, 8632 (1996).

[2] S. Jandl, P. Dufour, P. Richard, V. Nekvasil, D. I. Zhigunov, S. N. Barilo, and S. V. Shiryaev, J. Lumin. **78**, 197 (1998).

[3] S. Jandl, P. Dufour, V. Nekvasil, D. I. Zhigunov, S. N. Barilo, and S. V. Shiryaev, Physica C **314**, 189 (1999).

[4] T. Strach, T. Ruf, M. Cardona, C. T. Lin, S. Jandl, V. Nekvasil, D. I. Zhigunov, S. N. Barilo, and S. V. Shiryaev, Phys. Rev. B **54**, 4276 (1996).

[5] W. E. Wallace, S. G. Sankar, and V. U. Rao, Struct. Bonding **33**, 1 (1977).

[6] R. Harley, *Spectroscopy of Solids Containing Rare Earth Ions*, edited by A. A. Kaplyanskii and R. M. Macfarlane (Elsevier, New York, 1987).

[7] E. T. Heyen, R. Wegerer, and M. Cardona, Phys. Rev. B **67**, 144 (1991).

[8] A. A. Martin, V. G. Hadjiev, T. Ruf, M. Cardona, and T. Wolf, Phys. Rev. B **58**, 14 211 (1998).

[9] A. A. Martin, T. Ruf, M. Cardona, S. Jandl, D. Barba, V. Nekvasil, M. Divis, and T. Wolf, Phys. Rev. B **59**, 6528 (1999).

[10] J. Mesot and A. Furrer, J. Supercond. **10**, 623 (1997).

[11] B. G. Wybourne, *Spectroscopic Properties of Rare Earth* (Wiley, New York, 1965).

[12] M. Guillaume, W. Henggeler, A. Furrer, R. S. Eccleston, and V. Trounov, Phys. Rev. Lett. **74**, 3423 (1995).

[13] T. Wolf, W. Goldacker, B. Obst, G. Roth, and R. Flükiger, J. Cryst. Growth **96**, 1010 (1989).

[14] C. T. Lin, A. M. Niraimathi, Y. Yan, K. Peters, H. Benders, E. Schrönherr, and E. Gmelin, Physica C **272**, 285 (1996).

[15] D. J. Newman and B. Ng, Rep. Prog. Phys. **52**, 699 (1989).

[16] V. Nekvasil, M. Diviš, G. Hilscher, and E. Holland-Moritz, J. Alloys Compd. **255**, 578 (1995).

[17] M. Diviš, V. Nekvasil, and J. Kuriplach, Physica C **301**, 23 (1998).

[18] J. P. Perdew, S. Burke, and M. Ernzerhof, Phys. Rev. Lett. **77**, 3865 (1996).

[19] P. Blaha, K. Schwarz, J. Luitz, WIEN97, Vienna University of Technology, 1997. Improved and updated Unix version of the original copyrighted WIEN-code by P. Blaha, K. Schwarz, P. Sormantin, and S. B. Trickey, Comput. Phys. Commun. **59**, 399 (1990).

[20] K. Schwarz, C. Ambosch-Draxl, and P. Blaha, Phys. Rev. B **42**, 2051 (1990).
[21] M. Richter, J. Phys. D **31**, 1017 (1998).
[22] P. Novak, Phys. Status Solidi B **198**, 729 (1996).
[23] J.-P. R. Wells, M. Yamaga, T. P. J. Han, H. G. Gallagher, and M. Honda, Phys. Rev. B **60**, 3849 (1999).
[24] D. Barba, S. Jandl, A. A. Martin, C. T. Lin, M. Cardona, and T. Wolf (unpublished).
[25] C. A. Morrison and R. P. Leavitt, *Hanbook of the Physics and Chemistry of Rare Earths*, edited by K.A. Gschneider, Jr. and L. Eyring (North-Holland, Amsterdam, 1982).
[26] M. Guillaume, P. Allenspach, W. Henggeler, J. Mesot, B. Roessli, U. Staub, P. Fischer, A. Furrer, and V. Trounov, J. Phys.: Condens. Matter **6**, 7963 (1994).
[27] W. E. Pickett, Rev. Mod. Phys. **61**, 433 (1989).
[28] R. Coehorn and K. H. J. Bushow, J. Appl. Phys. **69**, 5590 (1991).
[29] K. N. Yang, J. M. Ferreira, B. W. Lee, M. B. Maple, W.-H. Li, J. W. Lynn, and R. W. Erwin, Phys. Rev. B **40**, 10 963 (1989).
[30] A. A. Nugroho, V. Nekvasil, I. Veltruský, S. Jandl, P. Richard, A.A. Menovsky, F.R. de Boer, and J.J.M. Franse, J. Magn. Magn. Mater. (to be published).
[31] V. N. Narozhnyi, D. Eckert, K. A. Nenkov, G. Fuchs, T. G. Uvarova, and K.-H. Muller, Physica C **312**, 233 (1999).
[32] T. Ruf, E. T. Heyen, M. Cardona, J. Mesot, and A. Furrer, Phys. Rev. B **46**, 11 792 (1992).
[33] W. E. Farneth, R. S. McLean, E. M. McCarron, F. Zuo, Y. Lu, B. R. Patton, and A. J. Epstein, Phys. Rev. B **39**, 6594 (1989).
[34] V. Likodimos, N. Guskos, H. Gamari-Seale, A. Koufoudakis, M. Wabia, J. Typek, and H. Fuks, Phys. Rev. B **54**, 12 342 (1996).